La Granja: Revista de Ciencias de la Vida
pISSN:1390-3799; eISSN:1390-8596
http://doi.org/10.17163/lgr.n39.2024.07

Scientific paper/ Artículo científico

Earth Sciences

Landslides Susceptibility Analysis employing Analytical Hierarchy Process on an Amazonian roadway in Ecuador

Análisis de Susceptibilidad a Deslizamientos empleando el Proceso de Jerarquía Analítica en una carretera amazónica del Ecuador

Cristian J. Cargua*[1], Ronny Espin[2], Bryan G. Valencia[3], Marco Simbaña[4], Sebastián Araujo[2], Carolina Cornejo[3] y Anderson Ocampos [2]

[1]*Universidad Nacional Mayor de San Marcos, Facultad de Ingeniería Geológica, Minera, Metalúrgica y Geográfica, Unidad de Posgrado, Lima, Perú.*
[2]*Grupo de Investigación en Geofísica y Geotecnia, Facultad de Ciencias de la Tierra y Agua, Universidad Regional Amazónica Ikiam, Muyuna Km 7, Tena, Napo, Ecuador.*
[3]*Grupo de Investigación de Ciencias de la Tierra y Clima, Facultad de Ciencias de la Tierra y Agua, Universidad Regional Amazónica Ikiam, Muyuna Km 7, Tena, Napo, Ecuador.*
[4]*Universidad de Investigación de Tecnología Experimental Yachay, Urcuquí, Ecuador.*

*Corresponding author: cristian.cargua@unmsm.edu.pe

Received on May 19th, 2022. Accepted, after review, on July 06th, 2023.

Abstract

The Puyo-Tena roadway is prone to landslides due to the geodynamics, geomorphology, and geological materials of the area (unstable outcrops and strata). In recent years, this problem has persistently caused the road to be partially or completely disabled on numerous occasions. The objective of the research was to generate a cartographic model of landslides susceptibility based on variables such as slope, geological formations, land cover and land use, as well as distances to faults, road, and rivers. The degree of landslides incidence was estimated as the linear combination of the weighted variables using the analytic hierarchy process. The importance of this semi-quantitative method lies in its ability to break down a complex decision problem into a simpler and more coherent decision model. The resulting cartographic model was classified into five susceptibility categories: very low, low, moderate, high, and very high. The results showed that 17 km out of the 80 km of the Puyo-Tena roadway have a high probability of landslides, which is equivalent to 21.25% of the road. Furthermore, within this percentage, it was determined that there are fifteen regions with a high probability of landslides due to their location in areas with steep slopes, porous and permeable lithology, a large number of rivers, and agricultural soils. The area under the curve (AUC) of the receiver operating characteristic (ROC) was used for model verification. The verification results showed that the cartographic model for the study area has an accuracy value of 83.7%. The cartographic model of landslide susceptibility will enable relevant decisions to be made to mitigate potential hazards that may endanger transporters, material goods, and residents of the area.

Keywords: susceptibility, landslide, analytical hierarchy process, geographic information system (GIS), susceptibility mapping model.

Resumen

La carretera Puyo-Tena es propensa a deslizamientos de tierra debido a la geodinámica, geomorfología y materiales geológicos de la zona (afloramientos y estratos inestables). En los últimos años, este problema ha provocado de forma persistente la inutilización parcial o total de la carretera en numerosas ocasiones. El objetivo de la investigación fue generar un modelo cartográfico de susceptibilidad a deslizamientos a partir de variables como la pendiente, las formaciones geológicas, la cobertura y uso de la tierra, así como las distancias a fallas, carretera y ríos. El grado de incidencia de deslizamientos se estimó como la combinación lineal de las variables ponderadas mediante el proceso de jerarquía analítica. La importancia de este método semicuantitativo radica en su capacidad para desagregar un problema de decisión complejo en un modelo de decisión más simple y coherente. El modelo cartográfico resultante se reclasificó en cinco categorías de susceptibilidad: muy baja, baja, moderada, alta y muy alta. Los resultados mostraron que 17 km de los 80 km de la carretera Puyo-Tena tienen una alta probabilidad a deslizamientos, lo que equivale a 21,25% de la carretera. Además, dentro de este porcentaje, se determinó que existen quince regiones con alta probabilidad de deslizamientos debido a su ubicación en zonas con fuertes pendientes, litología porosa y permeable, gran cantidad de ríos y suelos agrícolas. Para la verificación del modelo se utilizó el área bajo la curva (en inglés AUC) de la característica operativa del receptor (en inglés ROC). Los resultados de la verificación mostraron que el modelo cartográfico para el área de estudio tiene un valor de precisión de 83,7%. El modelo cartográfico de susceptibilidad a deslizamientos permitirá tomar las decisiones pertinentes para mitigar eventos potenciales que puedan poner en peligro a transportistas, bienes materiales y residentes de la zona.

Palabras clave: susceptibilidad, deslizamiento, proceso de jerarquía analítica, sistema de información geográfica (SIG), modelo cartográfico de susceptibilidad.

Suggested citation: Cargua, C., Espin, R., Valencia, B., Simbaña, M., Araujo, S., Cornejo, C. y Ocampos, A. (2023). Landslides Susceptibility Analysis employing Analytical Hierarchy Process on an Amazonian roadway in Ecuador. *La Granja: Revista de Ciencias de la Vida.* [Accepted version] http://doi.org/10.17163/lgr.n39.2024.07.

Orcid IDs:

Cristian J. Cargua: https://orcid.org/0000-0003-3036-270X
Ronny Espin: https://orcid.org/0000-0003-0409-4764
Bryan G. Valencia: https://orcid.org/0000-0002-5970-4964
Marco Simbaña: https://orcid.org/0000-0003-2974-3839
Sebastián Araujo: https://orcid.org/0000-0002-9704-5779
Carolina Cornejo: https://orcid.org/0000-0002-4421-1032
Anderson Ocampos: https://orcid.org/0000-0003-4094-2337

1 Introduction

Landslides are characterized as mass movements of rocks, soil and debris down the slope under the direct influence of gravity (Cruden, 1991; Cruden and Varnes, 1996). These movements are part of the geological dynamics of the planet influenced by human activities, rains or static overloads, causing them to accelerate and in some cases be catastrophic (Pourghasemi et al., 2018; Basu and Pal, 2020). Landslide susceptibility indicates how likely a specific area is to fail, either locally or regionally (Hearn and Hart, 2019). This susceptibility is usually expressed with a landslide susceptibility mapping model showing the probability of landslide occurrence, regardless of the time scale. The relevance of these mapping models is that their development is specific and detailed about a particular area.

Mapping to determine landslide susceptibility analyzes variables that affect soil stability such as geology, geomorphology, topography and distance to rivers (Raghuvanshi et al., 2014; Dahal and Dahal, 2017; Hamza and Raghuvanshi, 2017; Vásquez, 2023). The development of susceptibility cartographic models considers data quality, spatial resolution of the work area and the methodology for the analysis and digitization of the variables used (Mansouri Daneshvar, 2014). The development of these models considers qualitative approaches (such as the heuristic method and the Mora-Charson-Mora method), quantitative approaches (such as the deterministic method and the statistical method) or the union of both. Historically, the first models to be developed consisted of qualitative data with geological and morphological aspects of landslides inventoried (Nilsen et al., 1979; Mallick et al., 2018). Progressively, they were further refined and included more robust analyzes such as analytical hierarchy analyzes (Komac, 2006; Tešić et al., 2020; Chanu and Bakimchandra, 2022), bivariate (Van Westen, 1997; Jamir et al., 2022), multivariate (Carrara, 1983; Benchelha et al., 2020; Pham et al., 2021), logistic regression(Dai et al., 2001; Lee and Min, 2001; Nhu et al., 2020; Wubalem and Meten, 2020), fuzzy logic (Ercanoglu and Gokceoglu, 2004; Bahrami et al., 2021; Bien et al., 2022) and artificial neural networks (Bragagnolo et al., 2020; Bravo-López et al., 2022; Gameiro et al., 2022).

Qualitative methods are characterized by incorporating expert opinion based on small-scale empirical results (Demir et al., 2013; Roccati et al., 2021; Asmare, 2023). In general, the most common qualitative methods are limited to analyzing the geological and geomorphological properties of landslides inventoried. However, there are more sophisticated qualitative methods such as semi-quantitative methods (Nicu and Asăndulesei, 2018; Dolui et al., 2019). A semi-quantitative method uses weighting and classification procedures in qualitative methods. A clear example is the analytical hierarchy process developed by Saaty (1990), which has been employed in this research. This method has become a widely used tool as it helps decision makers to choose the best criterion, reducing complex decisions to a series of comparative pairs and synthesizing the results (Sonker et al., 2021). Hence, this tool has been widely used by several researchers in the world for developing mapping models for landslide susceptibility (Guillen et al., 2022; Ozturk and Uzel-Gunini, 2022; Salcedo et al., 2022; Wang et al., 2022; Okoli et al., 2023).

A characteristic of the Amazon region of Ecuador is the frequency of landslides around major towns and major road networks (Gobierno Cantonal de Pastaza, 2020; Gobierno Provincial de Napo, 2020; Secretaría Técnica de la Circunscripción Territorial Especial Amazónica , 2021; Servicio Nacional de Gestión de Riesgos y Emergencias, 2022a,b). However, the low spatial resolution of the susceptibility models available at regional scale prevents to know the susceptibility of point areas (Zumpano et al., 2014). For example, the Puyo-Tena highway, located between the provinces of Pastaza and Napo, does not have detailed studies by the decentralized autonomous governments regarding the susceptibility to landslides as seen in the reports of the Gobierno Cantonal de Pastaza (2020) and the Gobierno Provincial de Napo (2020). This road often presents constant landslides that have affected the road between both provinces (Ecoamazónico, 2014, 2020, 2021; Correo, 2017; Obras Públicas Ecuador , 2022). Therefore, this research aims to generate a landslide susceptibility mapping model that identifies the regions most prone to landslides along the Puyo-Tena road. The route is considered an important network connecting Ecuador with its Amazon region.

2 Study Area

The research was carried out on the Puyo-Tena highway, between the provinces of Pastaza and Napo, in the Ecuadorian Amazon (Figure 1). The road is bounded to the west by the Cordillera Real, to the north by the canton Tena, to the east by the Basin Oriente and to the south by the province of Pastaza. In addition, it has a wide variety of landforms such as mountainous regions, slopes and plains (Ministerio del Ambiente de Ecuador, 2014).

The aspects that comprise the study area are slope (from 5° to >70°), altitude (from 449 meters above sea level (hereinafter m.a.s.l) to 1108 m.a.s.l), precipitation (from 3500 mm/year to 4500 mm/year) and residual soils. In addition, the area of interest has an average annual temperature of 23.5°C and an annual precipitation of 4200 mm (Harris et al., 2020). Certain areas of the slopes studied lack vegetation cover, porous lithology and heavy rainfall, develop ideal conditions for high infiltration rates, making them susceptible to landslides and soil erosion (Laraque et al., 2004; Bravo et al., 2017).

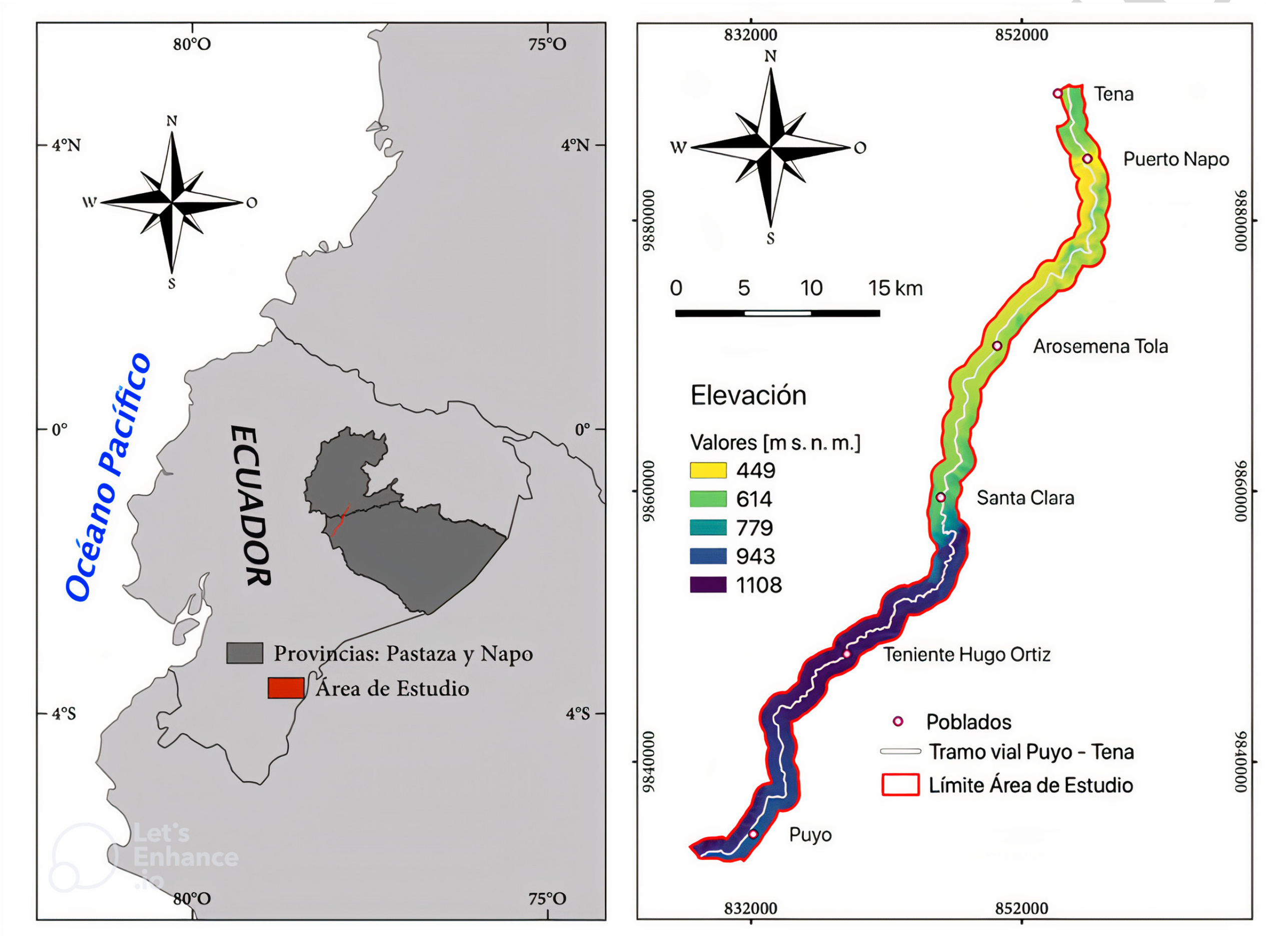

Figure 1. Location of the study area.

3 Materials and Methods

The Analytical Hierarchy Process (AHP) was used. AHP is a semi-quantitative method based on the evaluation of multi-criteria decision-making to treat complex and multi-attribute problems (Gudiyangada Nachappa et al., 2020). The analytical hierarchy process developed by Saaty (1990) disaggregates a complex decision problem at different hierarchical levels and allows to quantify opinions and transform them into a coherent decision model. The process is based on four principles: (i) hierarchy development, (ii) peer comparison, (iii) judgment synthesis and (iv) consistency check. This method along with the weighted linear combination allows to have the graphical representation of the most susceptible zones to landslide. In the end, the process of analytical hierarchy confers the best choice for the decision-making (Mallick et al., 2018; Basu and Pal, 2020; Zhou et al., 2020). The process leading to the landslide susceptibility mapping model is detailed below.

3.1 Landslide Inventory

According to Wieczorek (1984), it is necessary to provide a landslide map to discern locations and specify landslides that have occurred with different spatial and temporal scales. Thus, a representative landslide database is a prerequisite for any landslide hazard or risk assessment (Varnes and International Association of Engineering Geology, 2021; Guzzetti et al., 1999); and a landslide susceptibility mapping model is no exception. Using orthophotographs as a base, landslides were identified which were later confirmed in the field by three days of travel (July 27th, 28th and 29th, 2021). In addition, as a result of the *in situ* tour other landslides were found. Each landslide found was georeferenced and characterized according to its lithology and type of landslide. In total, 62 landslides were identified along the highway of interest. The largest slides are shown in Table 1 and Figure 2.

Table 1. Representative part of the inventory of landslides found on the Puyo-Tena road.

Inventory	Degree-Decimal Coordinates		Geological Formation	Slide Type
	Longitude	Latitude		
1	−77.8088°	−1.1159°	Arajuno	Rotational
2	−77.7947°	−1.0978°	Chalcana	Fall
3	−77.7933°	−1.0936°	Chalcana	Fall
4	−77.7905°	−1.0831°	Chalcana	Rotational
5	−77.7912°	−1.0789°	Tiyuyacu	Rotational

3.2 Preparation of the Layers of the Sliding Variables

All the information was collected from governmental and educational sources. This information is listed in Table 2. The variables to be considered in the susceptibility to landslides were geological formations, slope, geological faults, road construction, distance to rivers and land cover and use (hereinafter CUT). The selection of the six variables and their categories was based on the information obtained in the field and office. Similar studies in the region support the importance of taking into account this type of variables in the development of landslide susceptibility mapping models (Klimeš and Rios Escobar, 2010; Ortiz and Martínez-Graña, 2018; Barella et al., 2019; Orejuela and Toulkeridis, 2020; Vásquez, 2023). Categories refer to the different divisions of each variable; for example, the Napo, Tena, and Mera formations are categories of the variable geological formations. Subsequently, the selected variables were converted into thematic layers as an initial step in the development of the mapping model of susceptibility.

All subject layers were rasterized with a pixel resolution of 12.5 m. All the weights made for the six variables and their categories were selected according to the analyzes carried out in the field and office. The reclassifications for each thematic layer were performed based on the data obtained from each variable. Subsequently, the thematic layers were combined, analyzed with the AHP, using the Weighted Linear Combination (WLC) which is an analytical and hybrid method (qualitative and quantitative) used in GIS to process raster layers (Feizizadeh and Blaschke, 2013).

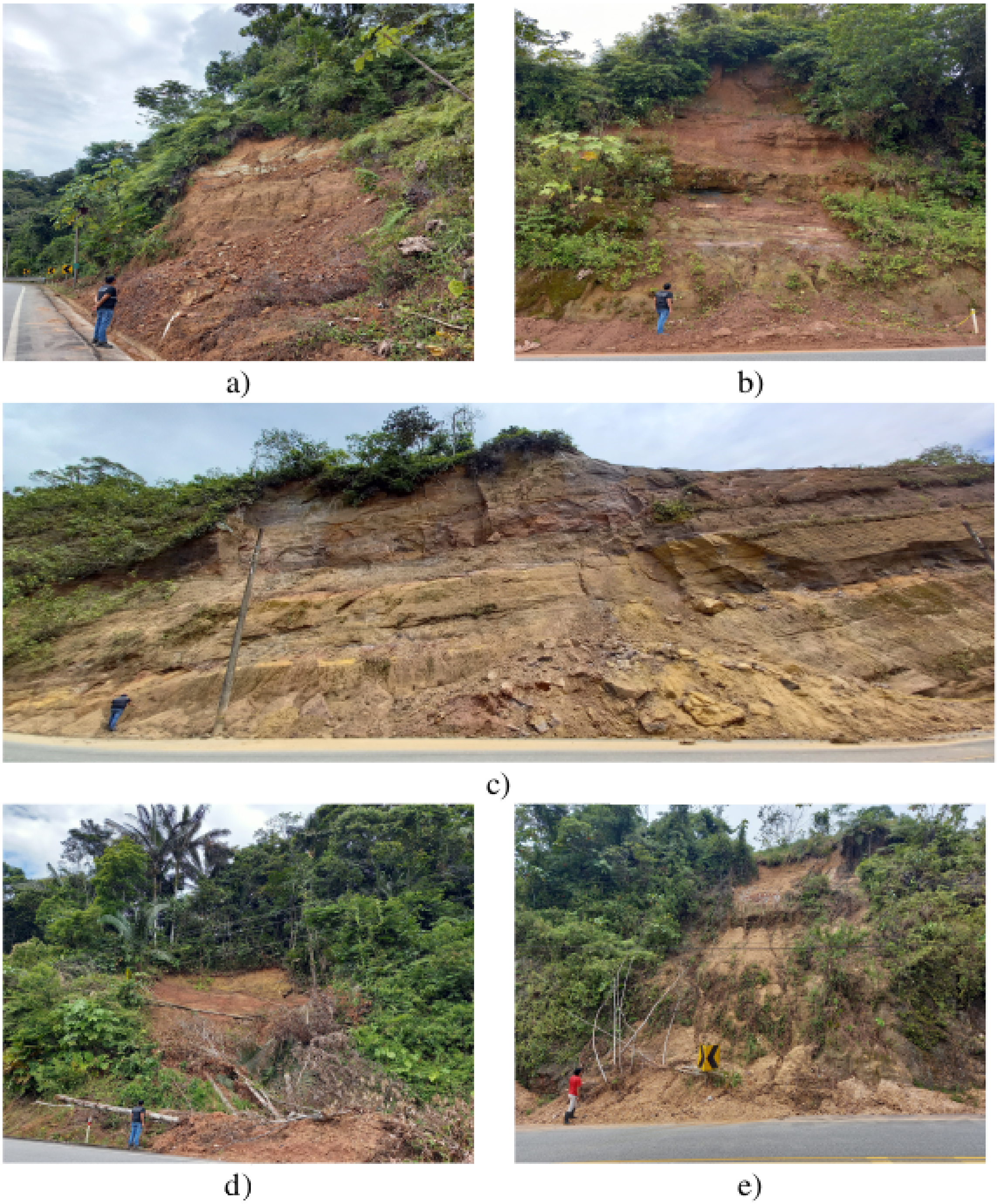

Figure 2. Landslides according to the inventory in Table 1: a) is 1, b) is 2, c) is 4, d) is 3 and e) is 5.

The distance to geological faults, roads and rivers were calculated using the buffer tool in QGIS. The slope was obtained from a Digital Elevation Model (DEM) of 12.5 m pixel resolution for the study area. All spatial analysis procedures were performed on the free software QGIS version 3.4 Madeira (Figure 3).

Table 2. Data sources used for the study.

Data	Description	Source
Orthophotos (Resolution 0.30 m)	Downloaded	SIGTIERRAS PROGRAM http://www.sigtierras.gob.ec/
Digital Elevation Model- DEM (Resolution 12.5 m)	Downloaded	ASF https://search.asf.alaska.edu/#/
Slope	Derived from the 12.5 m DEM	DEM 12.5 m
Geological Formations	Downloaded	MAGAP http://geoportal.agricultura.gob.ec/
Geological Faults	Downloaded	SARA PROJECT https://sara.openquake.org/start
Roads	Downloaded	IGM http://www.geoportaligm.gob.ec/portal/
Rivers	Downloaded	IGM http://www.geoportaligm.gob.ec/portal/
Land Cover and Land Use (CUT)	Downloaded	MAGAP http://geoportal.agricultura.gob.ec/

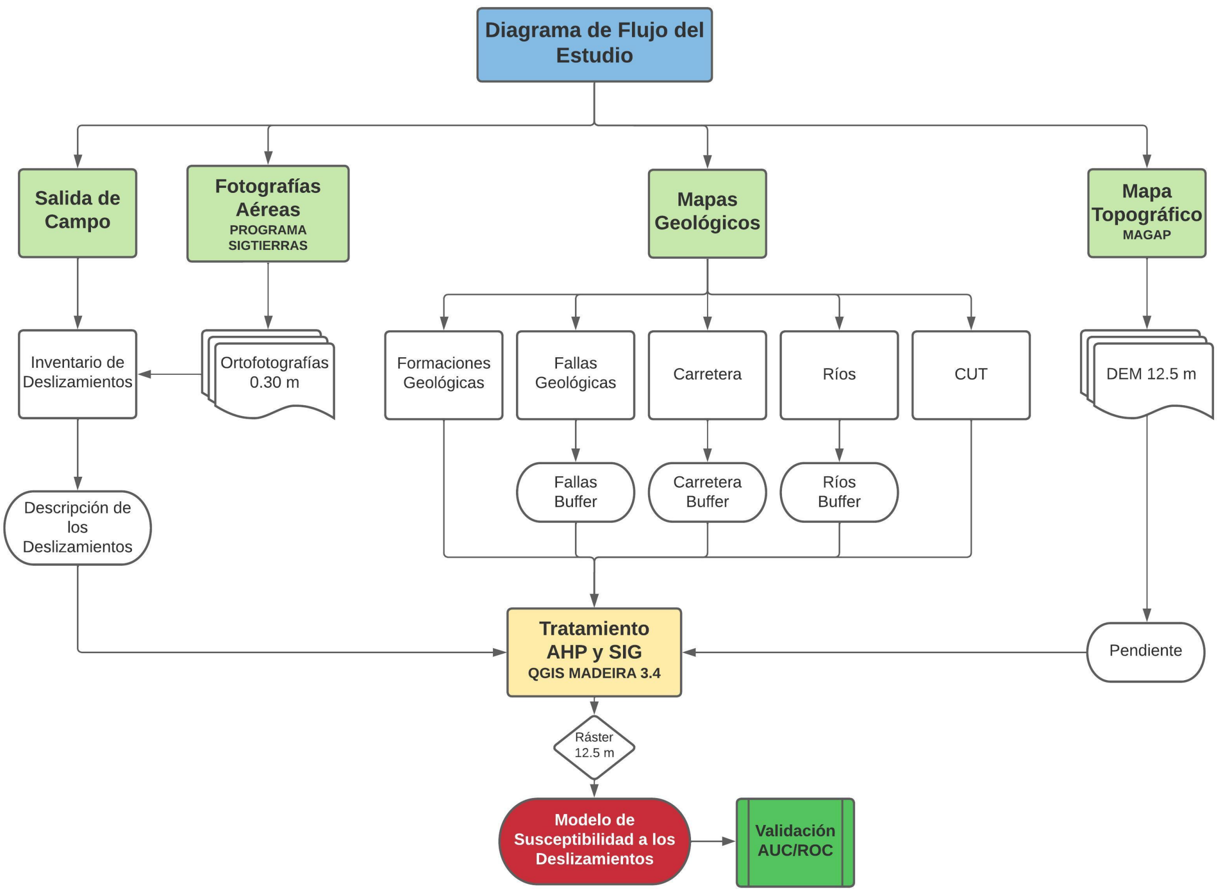

Figure 3. Flow Chart of the Study.

All vector subject layers were rasterized with pixel resolution of 12.5 m × 12.5 m. Rasterization allowed the six thematic layers to be combined and form a single raster layer. The pixel resolution of 12.5 m was selected because the DEM was worked with this spatial resolution. The procedure for each of the variables is detailed below.

Slope

The slope values were extracted from the DEM of 12.5 m pixel resolution. The slope is an indispensable variable, since depending on its inclination angle it will cause that there is greater or lesser susceptibility to landslides (Dolui et al., 2019; Nguyen et al., 2019; Bahrami et al., 2021). In this study, this topic layer was obtained using the QGIS gdaldem library; and it was categorized into six parts: $< 5°$, 5– 12°, 12– 25°, 25– 40°, 40– 70° y >70° (Figure 4a). The categorization was based on the reclassification established by the data source (Table 2). The weight values and the other variables are detailed in the results.

Geological Formations

Geological formations depending on lithology, permeability and soil consolidation will greatly influence the likelihood of landslides (Althuwaynee and Pradhan, 2017; Salehpour Jam et al., 2021). For developing this thematic layer, a total of seven geological formations, alluvial deposits, colluvial deposits and others (without description) along the road of interest were recorded (Figure 4b). The categorization was based on observations from recent formations and deposited.

Distance to Geological Faults

Areas with active faults are susceptible to landslides (Demir et al., 2013; Ozdemir, 2020). The areas closest to this area are more likely to occur due to landslides, due to intense shear. For developing this thematic layer, distances to failure were categorized into five classes: <200 m, 200- 400 m, 400- 600 m, 600-1000 m and >1000 m (Figure 4c). This categorization was based on observations of outcrops affected by the fault zones, which appeared up to 1000 m. In addition, the faults present in the study area correspond to quaternary faults, approximately <1.8 Ma.

Distance to Road

Roads located in slope areas condition that there is greater susceptibility to landslides, due to the presence of infrastructure, colonization process, emergence of new settlements and connections with other roads (Igwe et al., 2020; Panchal and Shrivastava, 2020). During the fieldwork, because of these four factors it was evident that there were outcrops affected located up to 750 m from the road line. For this reason, this thematic layer was categorized into four classes: <250 m, 250- 500 m, 500- 750 m and >750 m (Figure 4d).

Distance to rivers

Rivers erode the terrain, thus favoring landslides (Achour et al., 2017; Tešić et al., 2020). In the field, landslides located up to 750 m measured from the margin of the rivers were evidenced. There was a higher number of landslides near rivers and a higher displacement mass, compared to more distant regions where there was a lower number of landslides. Therefore, for this thematic layer, rivers were categorized into five classes: <50 m, 50- 250 m, 250-500 m, 500- 750 m and >750 m (Figure 4e).

Land Cover and Use (CUT)

The CUT is an important variable involved in landslide processes. The removal of forests to convert them into grasslands, agricultural areas or areas of urban expansion, intensifies the erosion and flow of flows when there is precipitation. These events largely favor the occurrence of landslides (Guevara et al., 2020; Roccati et al., 2021). For the development of this last thematic layer, five land use categories were registered: Agriculture, Area without Vegetation Cover, Forest, Shrub Vegetation and Anthropic Zone (Figure 4f). Water bodies were excluded because they were analyzed in the distance to rivers variable.

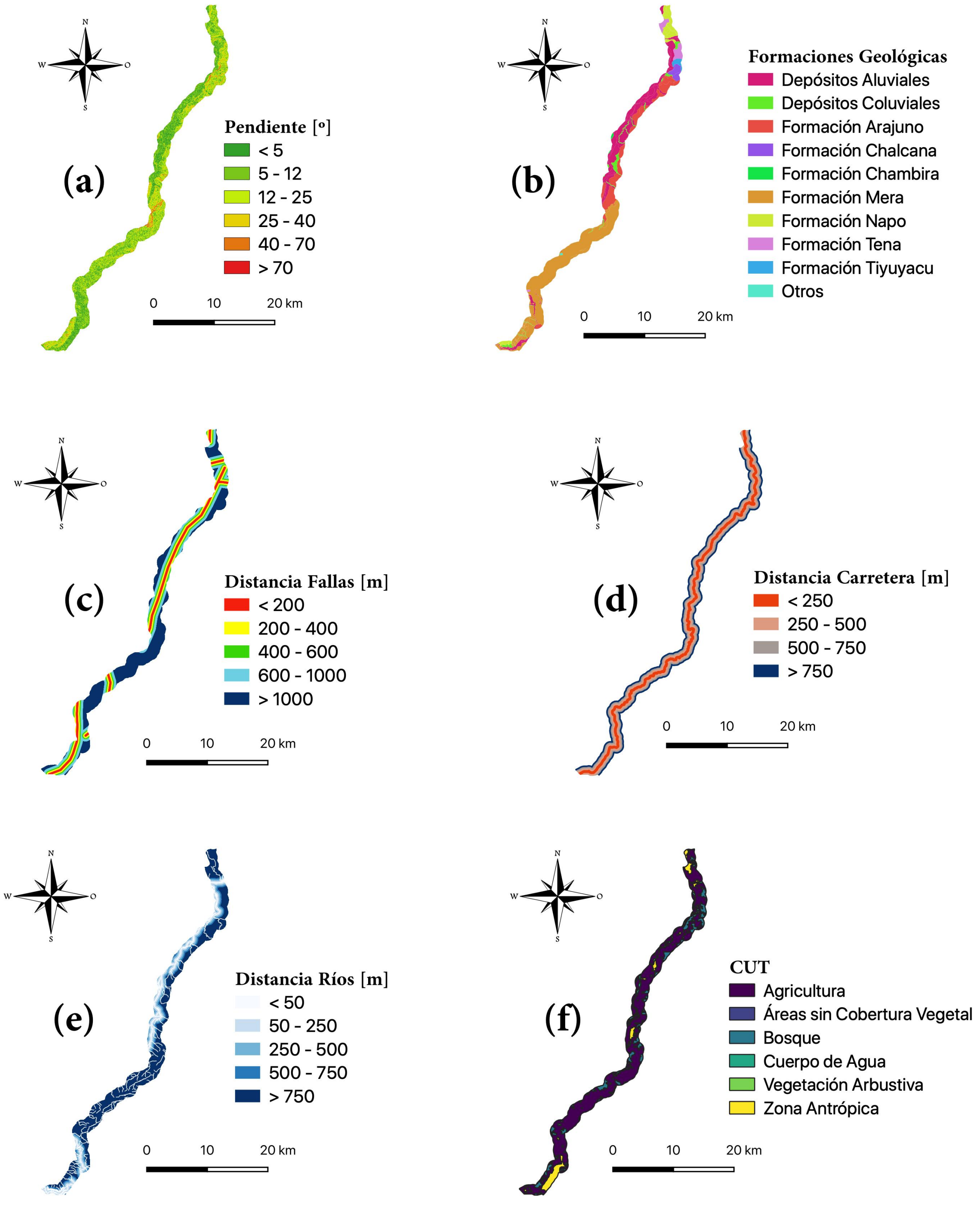

Figure 4. Thematic layers of variables along the Puyo - Tena road: (a) Slope, (b) Geological Formations, (c) Distance to Faults, (d) Distance to Road, (e) Distance to Rivers and (f) CUT.

3.3 Susceptibility Mapping

For the application of the AHP method, it is essential to assign a relative weight to the variables. Mathematical calculations to obtain the values of each step of the AHP were performed using the RStudio software. The steps used are described in detail below. a) Development of the hierarchical structure of the variables. b) Matrix of judgments by pair comparison. Relative weight according to Table 3 (Saaty, 1977). Applying the criterion of this table, it was decided which variable is more influential in relation to another variable. Priority was established and the six variables were weighted. (c) Synthesis of comparative judgements. Calculation of the final priority of each variable according to the table (Saaty, 1977). At this point the final normalized weighting of each variable was obtained, thus determining how much the variables contributed to meet the objective. d) Consistency evaluation. It allowed to verify if the weights of the comparative judgments had logic. e) Combination of thematic layers and obtaining the mapping model of susceptibility. f) Reclassification of the final mapping model of susceptibility.

Table 3. Fundamental Scale of Saaty (1977).

Value	Definition	Explanation
1	Equally important	Two decision items influence the main decision item equally.
3	Moderately more important	One decision element is moderately more influential than another.
5	Much more important	One decision element has more influence than another.
7	Really much more important	One decision-making element has a significantly greater influence than the other.
9	Extremely important	The difference in decision between the influences of the two decision elements is extremely significant.
2, 4, 6, 8	Intermediate Judgment Values	Values of judgment among equals, moderately, much, and extremely.

Once the weights were made, using the calculation of coherence or radius of coherence (*CR*), it was determined whether the calculation concluded correctly or not, described in the Eq (1). Thus, it was possible to recognize if there was coherence in the comparison of importance range of each variable.

$$CR = \frac{CI}{RI} \tag{1}$$

Where, *RI* (Table 4) refers to the random consistency index; instead,*CI* refers to the consistency index, described in Eq (2). The *RI* index is a defined value that is part of the AHP method.

$$CI = \frac{\lambda_{max} - n}{n-1} \tag{2}$$

Where,λ_{max} is the eigenmaximum value and is calculated from the array and *n* is the order of the array. According to Saaty (1990), the coherence ratio must be less than or equal to 10% or an imprecision of less than 10%. The principle is to compare judgment with random comparison of elements. Finally, the weights integrated the different causal classes in a single index of susceptibility to landslides, LSI using the Eq (3) (Saaty, 1990).

$$LSI = \sum_{i=1}^{n} R_i * W_i \tag{3}$$

Where, R_i are the classification classes of each variable and W_i are the weights for each of the conditioning variables of the landslides. The resulting cartographic model *LSI* was reclassified into five susceptibility classes: very low, low, moderate, high, and very high. These five divisions were made according to the method of quantiles using the pixel values of the final cartographic model of susceptibility to landslides.

3.4 Validation of the Cartographic Model

An adequate validation is obtained by comparing the final mapping model, developed from the AHP method with the landslide inventory map (Basu and Pal, 2020; Ozdemir, 2020). The validation was performed using the Receiver Operating Characteristics (*ROC*) method, which has been widely used for this type of studies (Igwe et al., 2020; Bahrami et al., 2021; Salehpour Jam et al., 2021; Kincal and Kayhan, 2022).

The ROC curve is used to graphically show the correlation between the true-positive rate and the false-positive rate (Soeters and Van Westen, 1996; Williams et al., 1999; Althouse, 2016). The area under the curve (AUC) of the ROC curve, the closer it is to 1.0, the better the prediction of the mapping model; however, the closer it is to 0.5, the more unreliable the model will have a random prediction.

Table 4. Index of Random Consistency of Saaty (1990).

n	1	2	3	4	5	6	7	8	9	10
RI	0	0	0.58	0.90	1.12	1.24	1.32	1.41	1.45	1.49

4 Results

4.1 Analytic Hierarchy Process

Hierarchy and pair comparison allowed to know the influence degree of the variables of landslides (Table 5). The most outstanding variables were slope, geological formations, distances to rivers and land cover and use, while the least influential were road distances and faults. The analysis of the coherence radius for each variable and for the final susceptibility cartographic model obtained a value lower than 0.10 (Table 5 and Table 6). These values reflect that the AHP procedure was performed correctly. After hierarchization, pair comparison, comparative judgments and consistency assessment, the final matrix was obtained with the weights of the six variables to make final landslide susceptibility model (Table 6).

The final landslide susceptibility model was reclassified into five classes: very low, low, moderate, high and very high (Figure 5). Based on data from the table (Table 7), the susceptibility area percentages were very low (0.64 %), low (31.96 %), moderate (50.87 %), high (15.83 %), and very high (0.70 %). Once the model was completed, it was found that there are fifteen regions in the Puyo-Tena road with high and very high susceptibility classes (Figure 5 and Table 8), where four of them are located near the towns of Puyo, Santa Clara, Arosemena Tola and Puerto Napo. The 15 regions were selected after observation and analysis of the final model. The inventoried landslides were placed on the final cartographic model and most of them were located within these fifteen regions of high and very high susceptibility to landslides.

4.2 Validation of the Cartographic Model

The "ROCR" library of the "ROCR" package was used in the RStudio software to evaluate the accuracy of our landslide susceptibility mapping model. Analysis of the ROC curve revealed an AUC of 0.837, indicating a predictive accuracy of 83.7 % (Figure 6). This metric is a reliable measure to evaluate the performance of the model in predicting landslides.

Table 5. Matrix of hierarchy and pairs comparison of variables.

Variables	Categories	Weighting Categories	Variables Weighting	Weights Categories	CR Variables
Geological Formations	Alluvial Deposit	2	7	0.039	0.0032
	Tena Formation	8		0.154	
	Mera Formation	7		0.135	
	Arajuno Formation	8		0.154	
	Chambira Formation	6		0.115	
	Napo Formation	5		0.097	
	Tiyuyacu Formation	6		0.115	
	Chalcana Formation	5		0.097	
	Coluviall Deposit	4		0.077	
	Otros	1		0.020	
Failures	<200	9	2	0.359	0.0011
	200 – 400	7		0.280	
	400 – 600	5		0.199	
	600 – 1000	3		0.120	
	>1000	1		0.039	
Slope	<5°	1	9	0.039	0.0028
	5 – 12°	2		0.077	
	12 – 25°	4		0.154	
	25 – 40°	5		0.193	
	40 – 70 °	8		0.308	
	>70°	6		0.230	
Distance to Roads	<250	7	3	0.411	0.0033
	250 – 500	5		0.294	
	500 – 750	3		0.176	
	>750	2		0.118	
Distance to Rivers	<50	9	6	0.375	0.0017
	50 – 250	7		0.292	
	250 – 500	4		0.167	
	500 – 750	3		0.125	
	>750	1		0.043	
CUT	Agriculture	7	5	0.368	0.0039
	Vegetation Uncovered Area	1		0.053	
	Forest	4		0.211	
	Shrub Vegetation	5		0.263	
	Anthropic Zone	2		0.105	

Table 6. Pair comparison matrix and final weighting of each landslide variable.

	Peer Comparison Matrix						Weighting	Final CR
	Slope	Geological Formations	Rivers	CUT	Roads	Failures		
Slopes	1.00						0.281	0.0039
Geological Formations	0.78	1.00					0.219	
Rivers	0.67	0.86	1.00				0.187	
CUT	0.56	0.72	0.84	1.00			0.157	
Roads	0.34	0.43	0.50	0.60	1.00		0.094	
Failures	0.23	0.29	0.34	0.40	0.67	1.00	0.063	

5 Discussion

In this research, the GIS-based AHP method was used as a multicriteria evaluation method to identify areas susceptible to landslides on the Puyo-Tena road. The data presented from the six variables show how they influence landslide susceptibility along the study road; similar situation was observed in Hepdeniz (2020) and Chanu and Bakimchandra (2022). As a result of hierarchization, peer weighting, comparative judgments and the value obtained in the consistency radius (CR <0.1), the weights made in the variables are reliable and were correctly performed. In addition, with the validation of the cartographic model using the area under the AUC curve of the ROC curve, 0.837 was obtained, supporting that the quality of the susceptibility landslide model is very good (Roy and Saha, 2019; Sonker et al., 2021).

Compared to similar studies carried out on roads in other countries, different results were observed than those obtained in this research. The Indian road studied by Panchal and Shrivastava (2022) showed a value close to our study, with an AUC of 0.825. On the other hand, the China-Pakistan road studied by Ali et al. (2019), obtained an AUC of 0.72, while the road studied in Algeria by Achour et al. (2017), achieved an AUC value of 0.66. This brief comparison reveals the variability of AUC values in studies conducted in different regions of the world. This variation will be related to the number of landslides inventoried and the quality of the final landslide susceptibility mapping model.

According to the 1000 m buffer analyzed along the study road, 16.53% (25.38 km^2) correspond to potential regions for landslides distributed 15.83% (24.31 km) in high and 0.70% (1.07 km) in very high susceptibility. The rest, approximately 83.57% (128.14 km^2) of the road, does not represent a great risk for a possible landslide.

Table 7. Areas of categories of the landslide susceptibility mapping model.

Susceptibility Categories	Area [km^2]	Area [%]
Very Low	0.97	0.64
Low	49.07	31.96
Moderate	78.10	50.87
High	24.31	15.83
Very High	1.07	0.70
Total	153.52	100%

According to the landslide susceptibility LSI mapping model (Figure 5) and the data shown in Table 8, approximately 17 km of approximately 80 km of the Puyo- Tena road are landslide susceptible, i.e., 21.25% of the road is landslide-susceptible. Once analyzed the variables *in situ* and digitally, it was determined that the four most important variables to intervene in landslide processes in this study site are slope, geological formations, distances to rivers and CUT; on the contrary, the remaining two variables, distance to road and distance to faults, are the ones that have less influence. For this research the analyzed variables have this hierarchy, but as He and Beighley (2008) mention, perhaps in other conditions and another area of study, the less influential variables could be more determinant. For example, if a road under construction is passing through steep mountains (Pourghasemi et al., 2012), or if the study area is near areas of active fault causing earthquakes (Abedini et al., 2017), they would be the main variables for landslide susceptibility.

Table 8. Main regions of the Puyo- Tena road with high and very high susceptibility to landslides.

Region	km [Home]	Degree-Decimal Coordinates		km [End]	Degree-Decimal Coordinates	
		Longitude	Latitude		Longitude	Latitude
1	0.125	-78.0500	-1.5088	3.692	-78.0236	-1.4993
2	14.163	-77.9987	-1.4235	14.275	-77.9988	-1.4225
3	29.018	-77.9238	-1.3486	29.329	-77.9224	-1.3465
4	36.498	-77.8880	-1.3119	36.765	-77.8858	-1.3111
5	38.933	-77.8822	-1.2963	39.679	-77.8840	-1.2914
6	41.097	-77.8897	-1.2853	42.424	-77.8898	-1.2746
7	44.583	-77.8886	-1.2569	48.331	-77.8821	-1.2304
8	56.780	-77.8547	-1.1634	57.653	-77.8511	-1.1568
9	59.150	-77.8425	-1.1470	60.820	-77.8328	-1.1361
10	63.517	-77.8169	-1.1197	63.938	-77.8137	-1.1217
11	66.121	-77.8053	-1.1076	66.700	-77.8018	-1.1042
12	67.864	-77.7920	-1.1051	68.886	-77.7947	-1.0973
13	70.238	-77.7901	-1.0871	70.937	-77.7916	-1.0812
14	72.836	-77.7904	-1.0657	73.655	-77.7912	-1.0597
15	75.536	-77.7966	-1.0459	76.381	-77.7951	-1.0391

Based on the results, it is determined that there are fifteen regions of the road with a high probability of landslides (Figure 5 and Table 8). Most of these regions are located outside the main towns except for regions 1, 6, 8 and 15, which are located near the towns of Puyo, Santa Clara, Arosemena Tola and Puerto Napo, respectively. Despite the proximity, it does not represent a latent risk to the inhabitants of these sectors. For this study, the slope is the most important variable because most of the landslides inventoried show features of being influenced by the upwelling inclination; similar scenario in the studies carried out by Dolui et al. (2019) and Bahrami et al. (2021).

Most landslides occur in areas with slopes >40°, specifically in the range of 40°- 70°. Geological formations are considered the second important incidence variable, since their lithological constitution, geomechanical resistance and porosity are involved in the occurrence of landslides. The physical conditions of each geological formation have different influences for the appearance of landslides. Geological formations, such as Chambira, Tiyuyacu, Mera, Tena and Arajuno, have porous lithology, low geomechanical resistance and low resistance to permeability; for this reason, they have a large number of landslides. Rivers are the third important variable. The different rivers cross different areas of high and low slope, thus favoring soil erosion and loss in soil resistance. Most landslides were found near the rivers, giving a clear idea that it is an important variable in landslide processes. Finally, CUT is also considered an important variable. Land-use change causes soil degradation, loss of mechanical strength, and increased water infiltration and therefore greater susceptibility to landslides. All these aspects are influenced by anthropic activities, which are clearly observed along the Puyo- Tena road. In contrast, the distance to the road and the distance to faults have the least influence on landslides. There is a lot of traffic in the road Puyo - Tena, but the movements originated by vehicles or human activities do not influence to a great extent the landslides.

Geological faults are triggers of earthquakes, which generate ground movements. Earthquakes in the Amazon are not too frequent compared to other regions of the country, and the effects have been slight (Rivadeneira et al., 2007). On the study road these earthquakes have low magnitude and little periodicity and do not have great impact for landslides. For this reason, these two variables are the ones that least influence the occurrence of landslides in the study area.

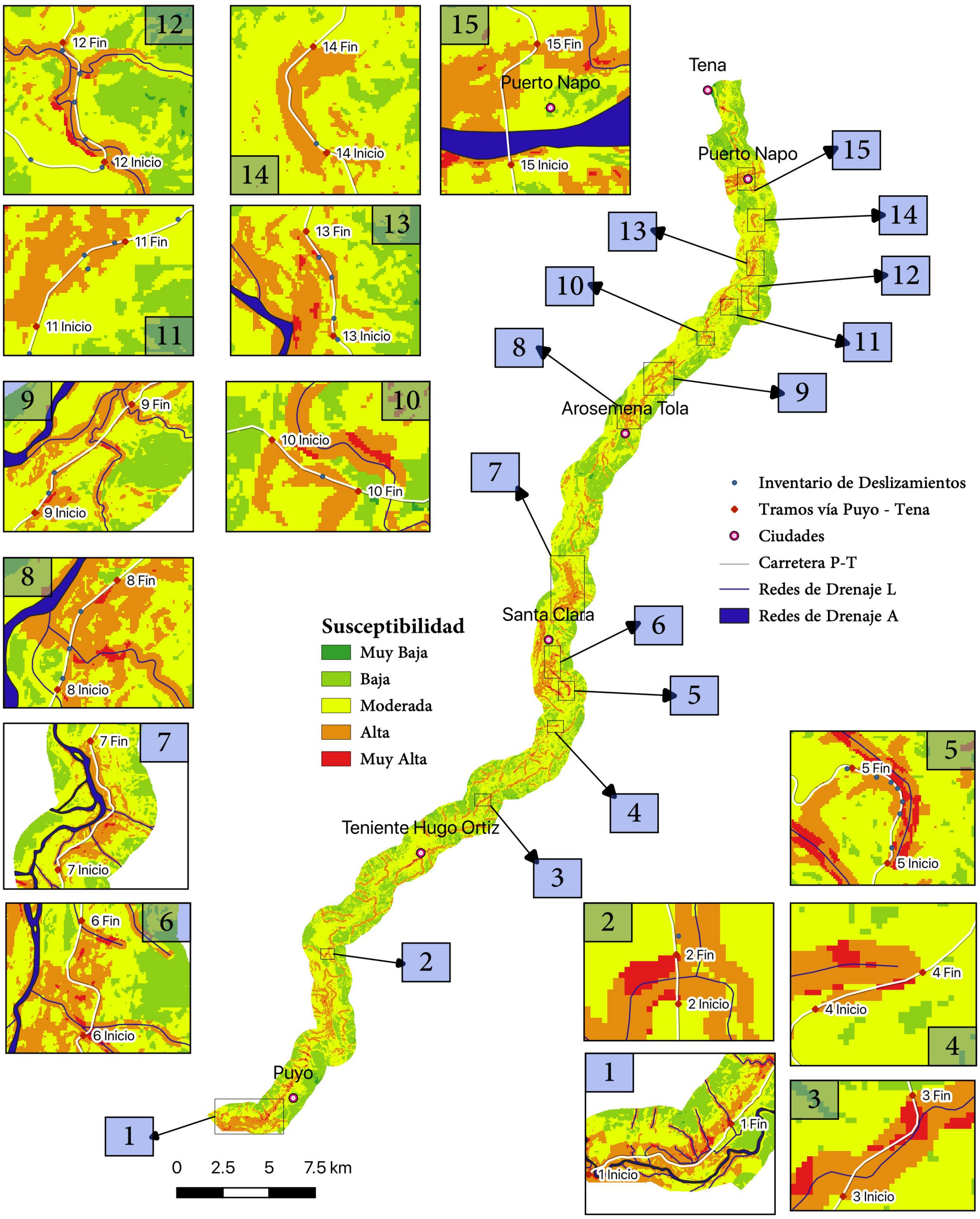

Figure 5. Landslide Susceptibility LSI cartographic model using the AHP method. Regions of the Puyo- Tena road.

Finally, new cartographic methods have been developed in recent decades for analyzing the susceptibility to landslides such as logistic regression, neural networks, *machine learning* and AHP, which is a method based on landslide inventories and statistical analysis, multicriteria, expert judgment, hierarchization, among others. Six variables that are commonly present in landslide processes were taken into account. The hierarchization of each of them was subject to the landslide inventory and the knowledge of the study area. From the four principles of the AHP method it was possible to obtain a mapping LSI model of susceptibility to landslides, and thus determine the main regions susceptible to landslides of the Puyo- Tena road.

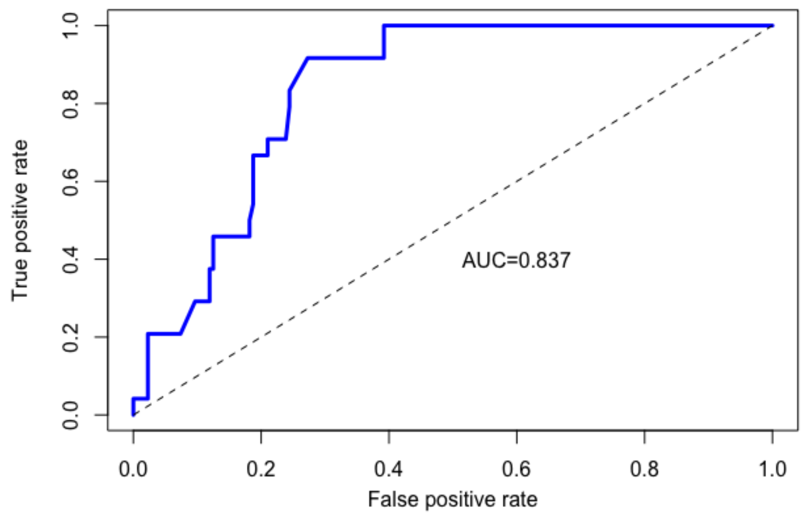

Figure 6. The ROC curve of the landslide susceptibility mapping model using the AHP method.

6 Conclusions

The susceptibility to landslides on the Puyo- Tena road, assessed by the AHP method, allowed a quick and practical manipulation of the physical data of the study area. The mapping LSI susceptibility model was obtained through the hierarchization, weighting and digitalization of the six variables involved in the research. Validation via the AUC/ROC method yielded a value of 0.837 corresponding to a predictive accuracy of 83.7%, supporting the quality of the cartographic model developed. The application of the AHP method allowed to identify the most influential variables, which were slope, geological formations, distances to rivers and land cover and use. Firsthand, the LSI model was reclassified into five susceptibility classes, obtaining surfaces of 0.64%, 31.96%, 50.87%, 15.83% and 0.70% for the classes of very low, low, moderate, high and very high, respectively. It was determined that approximately 17 km of the approximately 80 km of the Puyo-Tena road are susceptible to landslides, i.e. 21.25% of the road has potential to landslides. In addition, it was known that the studied road has 15 regions between high and very high probability for landslides. These regions were located on areas of high slope, porous and permeable lithology, a large number of rivers and soils suitable for agriculture. In addition, regions 1, 6, 8 and 15 were located near the towns of Puyo, Santa Clara, Arosemena Tola and Puerto Napo, respectively. These regions, despite their proximity to the towns, apparently do not represent a risk to the inhabitants of the sector.

The landslide susceptibility mapping model provides information consistent with the landslide inventory collected in the field. This model can be operated by governmental or non-governmental institutions that aim at land use planning and land management or similar purposes. The susceptibility model will allow decisions to avoid potential dangers that threaten the life and well-being of the population, plan an efficient road network, consider the best options for urban and rural expansion, including developing construction policies adjacent to the roads.

References

Abedini, M., Ghasemyan, B., and Rezaei, M. (2017). Landslide susceptibility mapping in bijar city, kurdistan province, iran: a comparative study by logistic regression and ahp models. *Environmental earth sciences*, 76:1–14. Online:https://n9.cl/ghgby.

Achour, Y., Boumezbeur, A., Hadji, R., Chouabbi, A., Cavaleiro, V., and Bendaoud, E. (2017). Landslide susceptibility mapping using analytic hierarchy process and information value methods along a highway road section in constantine, algeria. *Arabian Journal of Geosciences*, 10:1–16. Online:https://n9.cl/ggext0.

Ali, S., Biermanns, P., Haider, R., and Reicherter, K. (2019). Landslide susceptibility mapping by using a geographic information system (gis) along the china–pakistan economic corridor (karakoram highway), pakistan. *Natural Hazards and Earth System Sciences*, 19(5):999–1022. Online:https://n9.cl/3qz9h.

Althouse, A. (2016). Statistical graphics in action: making better sense of the roc curve. *International Journal of Cardiology*, 215:9–10. Online:https://n9.cl/hipk6.

Althuwaynee, O. and Pradhan, B. (2017). Semi-quantitative landslide risk assessment using gis-based exposure analysis in kuala lumpur city. *Geomatics, Natural Hazards and Risk*, 8(2):706–732. Online:https://n9.cl/44j52.

Asmare, D. (2023). Application and validation of ahp and fr methods for landslide susceptibility mapping around choke mountain, northwestern ethiopia. *Scientific African*, 19:e01470. Online:https://n9.cl/7vjlh.

Bahrami, Y., Hassani, H., and Maghsoudi, A. v. (2021). Landslide susceptibility mapping using ahp and fuzzy methods in the gilan province, iran. *GeoJournal*, 86:1797–1816. Online:https://n9.cl/frz7v.

Barella, C., Sobreira, F., and Zêzere, J. (2019). A comparative analysis of statistical landslide susceptibility mapping in the southeast region of minas gerais state, brazil. *Bulletin of Engineering Geology and the Environment*, 78:3205–3221. Online:https://n9.cl/z8lcl2.

Basu, T. and Pal, S. (2020). A gis-based factor clustering and landslide susceptibility analysis using ahp for gish river basin, india. *Environment, development and sustainability*, 22:4787–4819. Online:https://n9.cl/uh67s2.

Benchelha, S., Aoudjehane, H., Hakdaoui, M., El Hamdouni, R., Mansouri, H., Benchelha, T., Layelmam, M., and Alaoui, M. (2020). Landslide susceptibility mapping in the commune of oudka, taounate province, north morocco: A comparative analysis of logistic regression, multivariate adaptive regression spline, and artificial neural network models. *Environmental & Engineering Geoscience*, 26(2):185–200. Online:https://n9.cl/fxlus.

Bien, T., Truyen, P. T., Phong, T., Nguyen, D., Amiri, M., Costache, R., Duc, D., Le, H., Nguyen, H., and Prakash, I. (2022). Landslide susceptibility mapping at sin ho, lai chau province, vietnam using ensemble models based on fuzzy unordered rules induction algorithm. *Geocarto International*, 37(27):17777–17798. Online:https://bit.ly/3QWPHxw.

Bragagnolo, L., da Silva, R., and Grzybowski, J. (2020). Landslide susceptibility mapping with r. landslide: A free open-source gis-integrated tool based on artificial neural networks. *Environmental Modelling & Software*, 123:104565. Online:https://n9.cl/2lss7i.

Bravo, C., Torres, B., Alemán, R., and Marín, H. (2017). Indicadores morfológicos y estructurales de calidad y potencial de erosión del suelo bajo diferentes usos de la tierra en la amazonía ecuatoriana. *Anales de Geografía de la Universidad Complutense*, 37(2):247–264. Online:https://n9.cl/2lss7i.

Bravo-López, E., Fernández Del Castillo, T., Sellers, C., and Delgado-García, J. (2022). Landslide susceptibility mapping of landslides with artificial neural networks: Multi-approach analysis of backpropagation algorithm applying the neuralnet package in cuenca, ecuador. *Remote Sensing*, 14(14):3495. Online:https://n9.cl/zihph.

Carrara, A. (1983). Multivariate models for landslide hazard evaluation. *Journal of the International Association for Mathematical Geology*, 15:403–426. Online:https://n9.cl/ij7ke.

Chanu, M. and Bakimchandra, O. (2022). Landslide susceptibility assessment using ahp model and multi resolution dems along a highway in manipur, india. *Environmental Earth Sciences*, 81(5):156. Online:https://n9.cl/55hjo.

Correo (2017). Tramos de 21 vías de once provincias siguen cerrados. Correo . Online:t.ly/sOAh .

Cruden, D. (1991). A simple definition of a landslide. *Bulletin of Engineering Geology & the Environment*, 43(1):27–29. Online:https://n9.cl/b5nhdd.

Cruden, D. and Varnes, D. (1996). *Landslides: investigation and mitigation*, chapter Chapter 3 - Landslide types and processes, pages 36–75. Transportation Research Board.

Dahal, B. and Dahal, R. (2017). Landslide hazard map: tool for optimization of low-cost mitigation. *Geoenvironmental Disasters*, 4:1–9. Online:https://n9.cl/xd5dr.

Dai, F., Lee, C., Li, J., and Xu, Z. (2001). Assessment of landslide susceptibility on the natural terrain of lantau island, hong kong. *Environmental geology*, 40:381–391. Online:https://n9.cl/pktic.

Demir, G., Aytekin, M., Akgün, A., Ikizler, S., and Tatar, O. (2013). A comparison of landslide susceptibility mapping of the eastern part of the north anatolian fault zone (turkey) by likelihood-frequency ratio and analytic hierarchy process methods. *Natural hazards*, 65:1481–1506. Online:https://n9.cl/4vxpj.

Dolui, B., Yuvaraj, R., and Geetha, G. (2019). Landslide susceptibility mapping using ahp model in nilgiri district. *Thematics Journal of Geography*, 8(12):189–208. Online:https://n9.cl/vy1ht.

Ecoamazónico (2014). Mtop atiende inmediatamente los 6 deslizamientos de tierra. Ecoamazónico. Online:http://t.ly/eezh .

Ecoamazónico (2020). Reporte de un derrumbe en la vía al tena. Ecoamazónico. Online:http://t.ly/n45D .

Ecoamazónico (2021). Vía habilitada en el paso lateral. Ecoamazónico. Online:http://t.ly/YDmXR .

Ercanoglu, M. and Gokceoglu, C. (2004). Use of fuzzy relations to produce landslide susceptibility map of a landslide prone area (west black sea region, turkey). *Engineering geology*, 75(3-4):229–250. Online:https://n9.cl/gyhr2c.

Feizizadeh, B. and Blaschke, T. (2013). Gis-multicriteria decision analysis for landslide susceptibility mapping: comparing three methods for the urmia lake basin, iran. *Natural hazards*, 65:2105–2128. Online:https://n9.cl/qlba92.

Gameiro, S., de Oliveira, G., and Guasselli, L. (2022). The influence of sampling on landslide susceptibility mapping using artificial neural networks. *Geocarto International*, pages 1–23. Online:https://n9.cl/qiex9x.

Gobierno Cantonal de Pastaza (2020). *Plan de Desarrollo y Ordenamiento Territorial del cantón Pastaza 2020-2030*. Gobierno Cantonal de Pastaza.

Gobierno Provincial de Napo (2020). *Plan de Desarrollo y Ordenamiento Territorial Napo 2020-2023*. Gobierno Provincial de Napo.

Gudiyangada Nachappa, T., Kienberger, S., Meena, S., Hölbling, D., and Blaschke, T. (2020). Comparison and validation of per-pixel and object-based approaches for landslide susceptibility mapping. *Geomatics, Natural Hazards and Risk*, 11(1):572–600. Online:https://n9.cl/bxnw9.

Guevara, M. d. J., Carbajal, N., and Tuxpan Vargas, J. (2020). Soil deterioration in the southern chihuahuan desert caused by agricultural practices and meteorological events. *Journal of Arid Environments*, 176:104097. Online:https://n9.cl/j313s.

Guillen, K., Mendoza, M., Macías, J., and Solis-Castillo, B. (2022). Landslide susceptibility analysis based on a semiquantitative method in the sierra-costa region, michoacán, mexico. *Physical Geography*, 43(4):463–486. Online:https://n9.cl/84ebbv.

Guzzetti, F., Carrara, A., Cardinali, M., and Reichenbach, P. (1999). Landslide hazard evaluation: a review of current techniques and their application in a multi-scale study, central italy. *Geomorphology*, 31(1-4):181–216. Online:https://bit.ly/3udcJaq.

Hamza, T. and Raghuvanshi, T. (2017). Gis based landslide hazard evaluation and zonation–a case from jeldu district, central ethiopia. *Journal of King Saud University-Science*, 29(2):151–165. Online:https://n9.cl/i8u6e.

Harris, I., Osborn, T., Jones, P., and Lister, D. (2020). Version 4 of the cru ts monthly high-resolution gridded multivariate climate dataset. *Scientific data*, 7(1):109. Online:https://n9.cl/6huao.

He, Y. and Beighley, R. (2008). Gis-based regional landslide susceptibility mapping: a case study in southern california. *Earth Surface Processes and Landforms: The Journal of the British Geomorphological Research Group*, 33(3):380–393. Online:https://n9.cl/977ea.

Hearn, G. and Hart, A. (2019). Landslide susceptibility mapping: a practitioner's view. *Bulletin of Engineering Geology and the Environment*, 78(8):5811–5826. Online:https://n9.cl/kvril.

Hepdeniz, K. (2020). Using the analytic hierarchy process and frequency ratio methods for landslide susceptibility mapping in isparta-antalya highway (d-685), turkey. *Arabian Journal of Geosciences*, 13(16):795. Online:https://n9.cl/dzcxg.

Igwe, O., John, U., Solomon, O., and Obinna, O. (2020). Gis-based gully erosion susceptibility modeling, adapting bivariate statistical method and ahp approach in gombe town and environs northeast nigeria. *Geoenvironmental Disasters*, 7:1–16. Online:https://n9.cl/9d7nz.

Jamir, M., Chang, C., Jamir, I., Thong, G., and Walling, T. (2022). Landslide susceptibility mapping of noklak town, nagaland, north-east india using bivariate statistical method. *Geological Journal*, 57(12):5250–5264. Online:https://n9.cl/q0qdk.

Kincal, C. and Kayhan, H. (2022). A combined method for preparation of landslide susceptibility map in izmir (türkiye). *Applied Sciences*, 12(18):9029. Online:https://n9.cl/u3cks.

Klimeš, J. and Rios Escobar, V. (2010). A landslide susceptibility assessment in urban areas based on existing data: an example from the iguaná valley, medellín city, colombia. *Natural Hazards and Earth System Sciences*, 10(10):2067–2079. Online:https://n9.cl/v4r15.

Komac, M. (2006). A landslide susceptibility model using the analytical hierarchy process method and multivariate statistics in perialpine slovenia. *Geomorphology*, 74(1-4):17–28. Online:https://n9.cl/gw7og.

Laraque, A., Ceron, C., Armijos, E., Pombosa, R., Magat, P., and Guyot, J. (2004). *ediment Transfer through the fluvial system*, volume 288, chapter Sediment yields and erosion rates in the Napo River Basin: an Ecuadorian Andean Amazon tributary, pages 220–225. Online:https://bit.ly/3MH0nOd. IAHS.

Lee, S. and Min, K. (2001). Statistical analysis of landslide susceptibility at yongin, korea. *Environmental Geology*, 40(9):1095–1113. Online:https://bit.ly/3tzABol.

Mallick, J., Singh, R., AlAwadh, M., Islam, S., Khan, R., and Qureshi, M. (2018). Gis-based landslide susceptibility evaluation using fuzzy-ahp multicriteria decision-making techniques in the abha watershed, saudi arabia. *Environmental Earth Sciences*, 77:1–25. Online:https://n9.cl/uuy8p.

Mansouri Daneshvar, M. (2014). Landslide susceptibility zonation using analytical hierarchy process and gis for the bojnurd region, northeast of iran. *Landslides*, 11(6):1079–1091. Online:https://n9.cl/2azojx.

Ministerio del Ambiente de Ecuador (2014). *Sistema de Clasificación de Ecosistemas del Ecuador Continental*. Ministerio del Ambiente de Ecuador.

Nguyen, V., Pham, B., Vu, B., Prakash, I., Jha, S., Shahabi, H., Shirzadi, A., Ba, D., Kumar, R., Chatterjee, J., and Bui, D. (2019). Hybrid machine learning approaches for landslide susceptibility modeling. *Forests*, 10(2):157. Online:https://n9.cl/2i4cc.

Nhu, V., Shirzadi, A., Shahabi, H., Singh, S., Al-Ansari, N., Clague, J., Jaafari, A., Chen, W., Miraki, S., Dou, J., Luu, C., Górski, K., Pham, B., Nguyen, H., and Ahmad, B. (2020). Shallow landslide susceptibility mapping: A comparison between logistic model tree, logistic regression, naïve bayes tree, artificial neural network, and support vector machine algorithms. *International journal of environmental research and public health*, 17(8):2749. Online:https://n9.cl/am82bp.

Nicu, I. and Asăndulesei, A. (2018). Gis-based evaluation of diagnostic areas in landslide susceptibility analysis of bahluieț river basin (moldavian plateau, ne romania). are neolithic sites in danger? *Geomorphology*, 314:27–41. Online:https://n9.cl/71hsz.

Nilsen, T., Wright, R., Geological, U., Vlasic, T., Spangle, W., and Spangle, W. (1979). *Relative slope stability and land-use planning. Selected examples from the San Francisco Bay region, California*. Ministerio del Ambiente de Ecuador.

Obras Públicas Ecuador (2022). Trabajamos con maquinaria y personal en coordinación con @gadpastaza y gad de santa clara debido a un deslizamiento en el sector. Twitte r. Online:http://t.ly/B3fX .

Okoli, J., Nahazanan, H., Nahas, F., Kalantar, B., Shafri, H., and Khuzaimah, Z. (2023). High-resolution lidar-derived dem for landslide susceptibility assessment using ahp and fuzzy logic in serdang, malaysia. *Geosciences*, 13(2):34. Online:https://n9.cl/43tlc.

Orejuela, I. and Toulkeridis, T. (2020). Evaluation of the susceptibility to landslides through diffuse logic and analytical hierarchy process (ahp) between macas and riobamba in central ecuador. In *2020 Seventh International Conference on eDemocracy y eGovernment (ICEDEG)*, pages 201–207.

Ortiz, J. and Martínez-Graña, A. (2018). A neural network model applied to landslide susceptibility analysis (capitanejo, colombia). *Geomatics, Natural Hazards & Risk*, 9(1):1106–1128. Online:https://n9.cl/hg8r7.

Ozdemir, A. (2020). A comparative study of the frequency ratio, analytical hierarchy process, artificial neural networks and fuzzy logic methods for landslide susceptibility mapping: Taşkent (konya), turkey. *Geotechnical and Geological Engineering*, 38:4129–4157. Online:https://n9.cl/w77582.

Ozturk, D. and Uzel-Gunini, N. (2022). Investigation of the effects of hybrid modeling approaches, factor standardization, and categorical mapping on the performance of landslide susceptibility mapping in van, turkey. *Natural Hazards*, 114(3):2571–2604. Online:https://n9.cl/f0ct7.

Panchal, S. and Shrivastava, A. (2020). Application of analytic hierarchy process in landslide susceptibility mapping at regional scale in gis environment. *Journal of Statistics and Management Systems*, 23(2):199–206. Online:https://n9.cl/7uzpk.

Panchal, S. and Shrivastava, A. (2022). Landslide hazard assessment using analytic hierarchy process (ahp): A case study of national highway 5 in india. *Ain Shams Engineering Journal*, 13(3):101626. Online:https://n9.cl/b2pkh.

Pham, Q., Achour, Y., Ali, S., Parvin, F., Vojtek, M., Vojteková, J., Al-Ansari, N., Achu, A., Costache, R., Khedher, K., and Anh, D. (2021). A comparison among fuzzy multi-criteria decision making, bivariate, multivariate and machine learning models in landslide susceptibility mapping. *Geomatics, Natural Hazards and Risk*, 12(1):1741–1777. Online:https://n9.cl/719xzd.

Pourghasemi, H., Pradhan, B., and Gokceoglu, C. (2012). Application of fuzzy logic and analytical hierarchy process (ahp) to landslide susceptibility mapping at haraz watershed, iran. *Natural hazards*, 63:965–996. Online:https://n9.cl/l2h6a.

Pourghasemi, H., Teimoori Yansari, Z., Panagos, P., and Pradhan, B. (2018). Analysis and evaluation of landslide susceptibility: a review on articles published during 2005–2016 (periods of 2005-2012 and 2013-2016). *Arabian Journal of Geosciences*, 11:1–12. Online:https://n9.cl/06bsn.

Raghuvanshi, T., Ibrahim, J., and Ayalew, D. (2014). Slope stability susceptibility evaluation parameter (ssep) rating scheme–an approach for landslide hazard zonation. *Journal of African Earth Sciences*, 99:595–612. Online:https://n9.cl/zxw0it.

Rivadeneira, F., Segovia, M., Alvarado, A., Egred, J., Troncoso, L., Vaca, S., and Yepes, H. (2007). *Breves fundamentos sobre los terremotos en el Ecuador*. Corporación Editora Nacional.

Roccati, A., Paliaga, G., Luino, F., Faccini, F., and Turconi, L. (2021). Gis-based landslide susceptibility mapping for land use planning and risk assessment. *Land*, 10(2):162. Online:https://n9.cl/oke3i.

Roy, J. and Saha, S. (2019). Landslide susceptibility mapping using knowledge driven statistical models in darjeeling district, west bengal, india. *Geoenvironmental Disasters*, 6(1):1–18. Online:https://n9.cl/ro35j.

Saaty, T. L. (1977). A scaling method for priorities in hierarchical structures. *Journal of mathematical psychology*, 15(3):234–281. Online:https://n9.cl/zvwbr.

Saaty, T. L. (1990). *The Analytic Hierarchy Process: Planning, Priority Setting, Resource Allocation*.

Analytic hierarchy process series. RWS Publications.

Salcedo, D., Padilla Almeida, O., Morales, B., and Toulkeridis, T. (2022). Smart city planning based on landslide susceptibility mapping using fuzzy logic and multi-criteria evaluation techniques in the city of quito, ecuador. In *Doctoral Symposium on Information and Communication Technologies - DSICT*, pages 89–103.

Salehpour Jam, A., Mosaffaie, J., Sarfaraz, F., Shadfar, S., and Akhtari, R. (2021). Gis-based landslide susceptibility mapping using hybrid mcdm models. *Natural Hazards*, 108:1025–1046. Online:https://n9.cl/in8wa.

Secretaría Técnica de la Circunscripción Territorial Especial Amazónica (2021). *Plan Integral para la Amazonía 2021-203*. Secretaría Técnica de la Circunscripción Territorial Especial Amazónica.

Servicio Nacional de Gestión de Riesgos y Emergencias (2022a). Informe de situación no. 45 – época lluviosa a nivel nacional - cierre. Technical report, Servicio Nacional de Gestión de Riesgos y Emergencias.

Servicio Nacional de Gestión de Riesgos y Emergencias (2022b). Informe nro. 136 - época lluviosa del 01 de enero al 22 de julio de 2022. Technical report, Servicio Nacional de Gestión de Riesgos y Emergencias.

Soeters, R. and Van Westen, C. (1996). Slope instability recognition, analysis and zonation. *Landslides: investigation and mitigation*, 247:129–177. Online:https://n9.cl/vma1z.

Sonker, I., Tripathi, J., and Singh, A. (2021). Landslide susceptibility zonation using geospatial technique and analytical hierarchy process in sikkim himalaya. *Quaternary Science Advances*, 4:100039. Online:https://n9.cl/czyzla.

Tešić, D., Đorđević, J., Hölbling, D., Đorđević, T., Blagojević, D., Tomić, N., and Lukić, A. (2020). Landslide susceptibility mapping using ahp and gis weighted overlay method: a case study from ljig, serbia. *Serbian Journal of Geosciences*, 6(1):9–21. Online:https://n9.cl/h2k7n.

Van Westen, C. (1997). *ILWIS Applications Guide*, chapter Statistical landslide hazard analysis, pages 73–84. The International Institute for Aerospace Survey and Earth Sciences.

Varnes, D. and International Association of Engineering Geology (2021). *Landslide hazard zonation: a review of principles and practice*. Unesco.

Vásquez, J. y Estrada, M. (2023). A comparative study of the bivariate statistical methods and the analytical hierarchical process for the assessment of mass movement susceptibility. a case study: The lm-116 road-peru. *Rudarsko-geološko-naftni zbornik*, 38(1):149–166. Online:https://n9.cl/u17f0.

Wang, Z., Ma, C., Qiu, Y., Xiong, H., and Li, M. (2022). Refined zoning of landslide susceptibility: a case study in enshi county, hubei, china. *International journal of environmental research and public health*, 19(15):9412. Online:https://n9.cl/kwqq4.

Wieczorek, G. (1984). Preparing a detailed landslide-inventory map for hazard evaluation and reduction. *Bulletin of the Association of Engineering Geologists*, 21(3):337–342. Online:https://n9.cl/d0l2y.

Williams, C., Lee, S., Fisher, R., and Dickerman, L. (1999). A comparison of statistical methods for prenatal screening for down syndrome. *Applied Stochastic Models in Business and Industry*, 15(2):89–101. Online:https://n9.cl/38to7.

Wubalem, A. and Meten, M. (2020). Landslide susceptibility mapping using information value and logistic regression models in goncha siso eneses area, northwestern ethiopia. *SN Applied Sciences*, 2:1–19. Online:https://n9.cl/pg3ik.

Zhou, S., Zhou, S., and Tan, X. (2020). Nationwide susceptibility mapping of landslides in kenya using the fuzzy analytic hierarchy process model. *Land*, 9(12):535. Online:https://n9.cl/a1cjp.

Zumpano, V., Paola, R., Balteanu, D., Hussin, H., Reichenbach, P., Bălteanu, D., Micu, M., and Sterlacchini, S. (2014). A landslide susceptibility analysis for buzau county, romania. *Rev. Roum. Géogr./Rom. Journ. Geogr*, 58(1):9–16. Online:https://n9.cl/ten7t.